Pion inelastic scattering to giant resonances and low-lying collective states in ^{118}Sn and ^{40}Ca

J. L. Ullmann, J. J. Kraushaar, T. G. Masterson, R. J. Peterson, R. S. Raymond,* and R. A. Ristinen
University of Colorado, Boulder, Colorado 80309

N. S. P. King, R. L. Boudrie, and C. L. Morris
Los Alamos National Laboratory, Los Alamos, New Mexico 87545

R. E. Anderson[†]
University of North Carolina, Chapel Hill, North Carolina 27514

E. R. Siciliano[‡]
University of Colorado, Boulder, Colorado 80309
and Los Alamos National Laboratory, Los Alamos, New Mexico 87545

A comparison of differential cross sections for inelastic scattering of 130 MeV positive and negative pions has been made for studying the giant resonance region in ^{118}Sn and ^{40}Ca. In addition, several of the low-lying collective states in each target were examined. Comparison to distorted wave impulse approximation calculations allowed collective deformation lengths βR and fractions of the energy-weighted sum rules to be extracted. For bound collective states, the strengths for π^+ and π^- were nearly equal, as has been found for other scattering probes. Giant quadrupole and dipole excitations in ^{40}Ca ($T=0$) had nearly equal π^+ and π^- sum rule strengths. Quadrupole and monopole excitations in ^{118}Sn near 14 MeV show about twice the π^- transition strengths compared to those for π^+, contrary to expectations from simple isoscalar models.

I. INTRODUCTION

The giant resonances in nuclei are fundamental modes of collective excitation in nuclear matter. They occur systematically over a wide range of nuclear masses, and have been excited by virtually every nuclear scattering probe. These giant resonances may be pictured macroscopically as bulk oscillations of the neutrons and protons in the nucleus, and are classified as isoscalar (neutrons and protons moving in phase) or isovector (neutrons and protons moving out of phase). Microscopically, a giant resonance is pictured as the superposition of many neutron and proton particle-hole excitations, with a grouping into isovector and isoscalar excitations.

Different projectiles can selectively probe the spin and isospin structure of giant resonances. For example, alpha particle scattering is predominately isoscalar without spin transfer, while longitudinal electron scattering equally populates isoscalar and isovector modes. Inelastic scattering of pions offers a specific means to examine the isospin content of these excitations due to the large amplitudes for π^-n and π^+p in contrast to π^+n and π^-p scattering.

Inelastic pion scattering provides a good probe of the neutron-proton (or equivalently, isospin) character of a transition because of a useful property of the pion-nucleon interaction. In the vicinity of the $T=\frac{3}{2}$, $J=\frac{3}{2}$ resonance in the π-nucleon cross section [the $\Delta(1232)$, a very broad resonance centered at about 180 MeV], the free π^+-p (or π^--n) cross section exceeds the π^+-n (or π^--p) cross section by a factor of 9. Although this ratio is modified in

nuclear matter, the asymmetry in the cross section provides a means of separating the neutron and proton components of a given transition. In fact, in light nuclei a π^+/π^- ratio approaching the free nucleon value of 9 has been observed for some transitions.[1]

The prominent isoscalar quadrupole (GQR) and monopole (GMR) resonances were believed to consist of nearly equal neutron and proton vibrations. The first GQR examined by the two-pion charge states showed, however, a great deviation from this symmetry.[2]

To understand better the systematics of collective state excitation by pions, we also studied pion inelastic scattering to low-lying collective states. These states are typically sharp and well resolved from any continuum background, and have been extensively studied with a variety of probes. The comparison of pion data for the low-lying excitations to that from other probes provides a reference for the interpretation of results for transitions that have been studied more extensively than the giant resonances.

A closed-shell self-conjugate nucleus, ^{40}Ca, and a closed-proton-shell nucleus, ^{118}Sn, provided targets for this experiment. Previous studies[3−5] of pion scattering have emphasized low-lying states in several nuclei, whereas this work represents the first study of both giant resonances and low-lying states in the same nucleus.

In ^{118}Sn, we observed the low energy octupole, quadrupole, and monopole giant resonance states, usually considered to be the isoscalar modes.[6] A previous study of the GQR in ^{89}Y has been reported[7,8] only for π^+, so the present work represents the first comparison of π^+ and

π^- giant resonance cross sections in a neutron-excess nucleus. Positive pion excitation of the giant resonance states of ^{40}Ca has been reported,[8,9] as have comparisons of both charge states in ^{12}C.[10] We observed in ^{40}Ca, with both charge states, an unresolved complex separable into the isoscalar GQR and the isovector GDR modes. For ^{118}Sn, we found a significantly greater π^- to π^+ cross section ratio than expected for pure isoscalar transitions.

The π^-/π^+ ratio we observed is surprising. Bohr and Mottelson[11] have predicted that there should be neutron-proton differences in isoscalar giant resonances in $T > 0$ nuclei due to the neutron excess, but detailed calculations of the ratio of strengths due to this excess predict it to be less than N/Z.[12,13] As will be shown, the isospin effects we observe are greater than expected from a collective picture, and the traditional methods of calculating collective excitations do not reproduce our observations.

II. EXPERIMENTAL METHOD

These measurements were made at the Energetic Pion Channel and Spectrometer (EPICS) at the Clinton P. Anderson Meson Physics Facility (LAMPF). The ^{118}Sn data were taken on two separate occasions about one year apart. For the first part of the experiment, the ^{118}Sn target was 150±5 mg/cm^2 thick and enriched to 97% isotopic purity. For the second part, ^{118}Sn and natural Ca targets were run simultaneously and events were separated by tracing the scattered pion trajectories back to the target. This second ^{118}Sn target was 270±8 mg/cm^2 thick and the natural calcium target was gold plated and had an average thickness of 239±15 mg/cm^2. During the second part, data were also taken on the low-lying states in ^{118}Sn, including the ground state.

An incident pion energy of 130 MeV was chosen to optimize the necessary muon rejection at forward angles by time of flight between plastic scintillators located before and after the spectrometer dipoles. This enables rejection of muons from pion decay occurring between the scattering target and the front detector. Scattering angles measured at the front detectors were compared with those at the focal plane to identify and reject pion decays inside the dipoles. In addition, redundant muon rejection was used in the second part of this experiment. This was accomplished with a graphite wedge after the focal plane trigger scintillator, followed by a veto scintillator.[14] The central momentum of the spectrometer was kept the same for the measurements of the high-lying states at all angles and the graphite thickness was chosen to range out the pions and let the muons pass through to the veto scintillator.

The target angle was always set to half the spectrometer angle. The resolution of 600 keV FWHM was dominated by the thickness of the target and first scintillator. A 3 deg angular acceptance in the scattering plane was used in the data analysis. A more complete description of the use of the EPICS apparatus is found in Ref. 15.

The data were normalized to $\pi^\pm$p scattering from a CH$_2$ target measured at one angle. Pi-nucleon cross sections were calculated from the phase shifts of Carter, Bugg, and Carter.[16] The relative pion beam normalization was taken from the primary LAMPF proton beam

toroid. This normalization procedure was consistent with that based on ion chamber readings. The π-nucleon cross section, pion survival fraction through the spectrometer, spectrometer solid angle, primary beam monitoring, and spectrometer wire chamber efficiencies, were estimated to contribute 3% each to the normalization uncertainty. The CH$_2$ target thickness contributed about 1%, the statistics of measuring the πp cross section 1.5%, and the uncertainty in the Ca or Sn target thickness also 1.5%. These add to an overall normalization uncertainty of 9.2% for Sn and 10.8% for Ca. The absolute ratio of π^- to π^+ cross sections at a given angle is determined to somewhat higher accuracy because of the cancellation of several common uncertainties such as target thickness and solid angle. The uncertainty in the ratio is about 7.8% for both targets before including the uncertainties due to extracting peak areas.

Sample spectra for ^{118}Sn and Ca are shown in Figs. 1 and 2. There are two main sources of uncertainty in extracting a peak area—estimating the continuum and determining the peak shape. We made the usual assumption of considering the giant resonances to be enhancements of a definite multipolarity above a slowly-varying continuum. The continuum is believed to be due to processes such as quasifree scattering, but can also include a small (< 2%) uniform muon contamination. We approximated the continuum by a straight line under the peaks of interest. Typically, different reasonable choices in the background level caused a 10% to 15% variation in the extracted peak area, although in spectra with good statistics this was 6% or less.

The continuum cross section under the giant resonance peaks exhibited a smooth monotonic decrease with increasing angle. For Ca, the π^+ and π^- continua were roughly equal, while in ^{118}Sn the π^- continua were higher than the π^+, as might be expected in a $N > Z$ nucleus. Both π^+ and π^- continua were slightly smaller in the second part of the experiment. This was due in part to better muon rejection and in part to placing the elastic
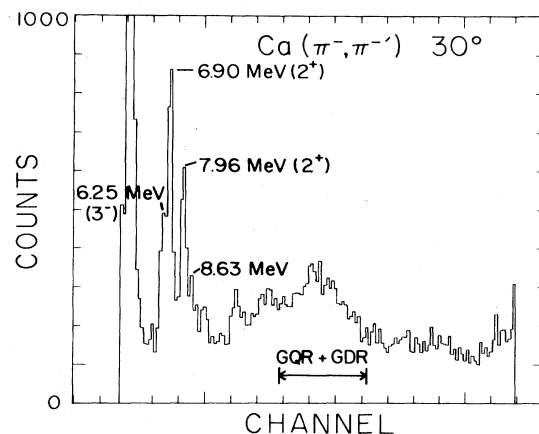

FIG. 1. Acceptance-corrected Ca($\pi^-,\pi^{-\prime}$) spectrum showing the low-lying states and giant resonance region. The energy region for the giant resonances was 15.2—22.0 MeV in excitation.
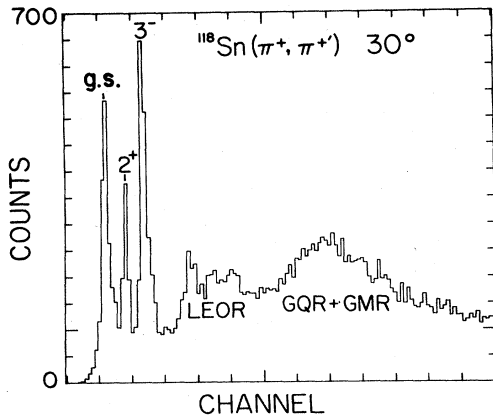
FIG. 2. Low-lying ^{118}Sn$(\pi^+,\pi^+{}')$ spectrum at 30° before acceptance correction.

peak off the focal plane and out of the spectrometer momentum acceptance, resulting in fewer decay muons in the spectrometer.

The shape of the giant resonances is in general a complicated distribution of particle-hole strength. However, in heavy nuclei, the macroscopic envelope of each resonance can be approximated by a single Gaussian shape. From measurements with other probes, the giant resonance region near 14 MeV in ^{118}Sn is known to consist of the giant quadrupole resonance at 13.2 MeV with a width of 3.8 MeV,[17] the isoscalar monopole resonance at 15.5 MeV with a width of 4.1 MeV,[17] the isovector dipole resonance at 15.6 MeV with a width of about 4.8 MeV (Ref. 18) and a smooth continuum. As shown in Fig. 3, the region was analyzed by fixing the energy and width of two Gaussians, one with the previously established parameters of the giant quadrupole resonance and the other at 15.5 MeV with a width of 4.4 MeV, and by determining a con-
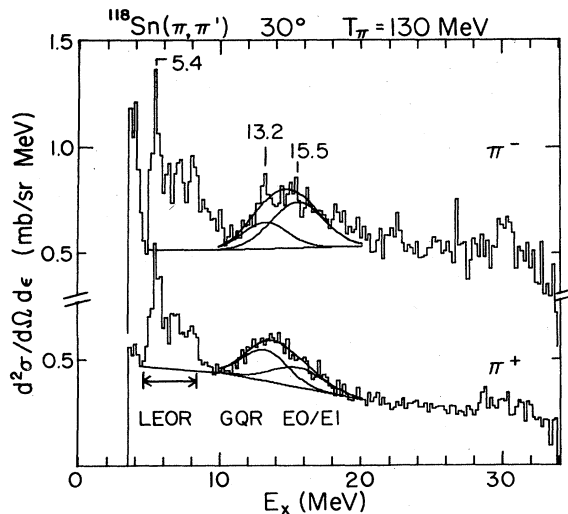

FIG. 3. Acceptance-corrected spectra for ^{118}Sn showing the region of the LEOR and the Gaussian decomposition of the giant resonance region.

sistent straight-line background. A detailed analysis of the fitting procedure was carried out for the 23° and 30° points. In general, the assumed widths were at or near the minimum of the χ^2 distribution. Varying one width while holding the other at its assumed value could cause as much as a 20% change in the measured area for a 0.4 MeV change in width, but typically this variation was less than 6%, and in some cases there was no variation. A Lorentzian shape, which can be used to describe isolated resonances and the giant dipole resonance, was also tried but not used because it could not simultaneously give good fits to both peaks and background.

We assumed a minimum contribution of 20% to the absolute cross section uncertainty for most peak areas to take into account uncertainties in the background and peak shape. For the ratio of cross sections at a given angle, this uncertainty would be somewhat less.

The giant resonance region in calcium could not be analyzed as overlapping Gaussians since the giant resonances in lighter nuclei tend to fragment and have non-Gaussian shapes. In particular, the (α,α') spectra of the giant quadrupole resonance obtained by Lui et al.[19] show a definite non-Gaussian shape with substantial strength on the high excitation side. For this reason, we treated the giant resonance region in Ca as a complex, and summed the spectra above a straight-line background from $E_x = 15.2$ to 22.0 MeV which was the same energy region used by Liu et al.[19] The two narrow peaks at lower excitation in the giant resonance region were fit by Gaussians.

III. DWIA CALCULATIONS

The data were analyzed in the framework of the distorted wave impulse approximation (DWIA). Calculations for elastic and inelastic scattering were made using the code DWPIES, a configuration-space code based on the code DWPI.[20] In this code, the same zero-range π-nucleon t matrix determines both the first-order elastic optical potential and the inelastic transition operator. The isoscalar and isovector parameters that characterize the t matrix are determined directly from the π-nucleon phase shifts of Rowe et al.[21] with no energy shift. The precise form of the optical potential is given in Ref. 22.

The π-nucleon interaction has s- and p-wave components at the beam energy used in this work. This can be written as

$$t_\phi(\vec{r}) \simeq \lambda_0 \rho_0(\vec{r}) + \phi \lambda_1 \rho_1(\vec{r}) ,\tag{1}$$

where $\phi = \pm 1$ for $\pi^\pm$, ρ_0 and ρ_1 denote the isoscalar and isovector transition densities, and λ_0 and λ_1 the isoscalar and isovector interaction parameters determined from the phase shifts. At energies near the $\Delta(1232)$ resonance, the p-wave interaction is dominant, and in this case $\lambda_0 \simeq 2\lambda_1$.

For all our calculations we used macroscopic derivative transition densities. Although microscopic transition densities are becoming available, we used the collective form for a more direct comparison to data obtained with other probes, most of which have been analyzed using the collective model. For all states except the giant monopole resonance, we used

$$\rho_i = B_i \frac{1}{\sqrt{2l+1}} \frac{\partial}{\partial r} \rho_{\text{g.s.}}(\vec{r}) Y_{l0}(\vec{r}) \, , \qquad (2)$$

where i equals 0 or 1 for the isoscalar or isovector term, $\rho_{\text{g.s.}}$ is the ground state distribution normalized to unity, and B_i is the isoscalar or isovector normalization constant that characterizes different nuclear models. For the isoscalar giant monopole resonance we used the particle-conserving breathing-mode transition density.[23]

$$\rho_i = B_i \left[3\rho_{\text{g.s.}} + \frac{\partial \rho_{\text{g.s.}}}{\partial r} \right] Y_{00}(\vec{r}) \, . \qquad (3)$$

The ground-state density used to calculate the distorted waves was taken as a two-parameter Fermi distribution with the half-density radius, c, and the diffuseness, a, taken from electron scattering[24] and corrected for the finite size of the proton. We used the same ground state parameters for the transition density and assumed that the neutron and proton distributions have the same shape and size. For ^{118}Sn, we used $c = 5.41$ fm and $a = 0.517$ fm, and for ^{40}Ca we used $c = 3.51$ fm and $a = 0.563$ fm. Equation (1) assumes that the isoscalar and isovector transition densities can be written simply as the sums or differences of neutron and proton distributions.

For the nominally isoscalar low-lying states and giant resonances, we made calculations based on two simple nuclear models to investigate the effects of the isovector part of the transition operator. For both models we set $B_0 = Z(\beta R)_p + N(\beta R)_n$ where βR is the proton or neutron deformation length. We assume $(\beta R)_p = (\beta R)_n = (\beta R)_0$, determined from an isoscalar energy-weighted sum rule as described later. In the first case we treat the isoscalar states as a pure isoscalar response and set $B_1 = 0$. This implies that the π^- and π^+ cross sections can differ only through the distorted waves. For the second case we assume the hydrodynamic model and set

$$B_1 = Z(\beta R)_p - N(\beta R)_n = (Z - N)(\beta R)_0 \, .$$

This is the model usually assumed for calculations involving other hadronic projectiles. For the giant quadrupole resonance in ^{118}Sn we also used the schematic model calculations of Brown and Madsen[12] which allow $(\beta R)_n$ and $(\beta R)_p$ to differ. This will be described later. For the giant dipole state, we assume a pure isovector response by setting $B_0 = 0$ and again used $B_1 = Z(\beta R)_p - N(\beta R)_n$. In this case, the derivative transition density corresponds to the Goldhaber-Teller model.[23]

Sensitivities of $(\beta R)^2$ to the assumed equality of the neutron and proton distributions were examined for ^{118}Sn in Ref. 2 and found to be slight. The use of a Tassie[25] form for the transition density, which weights the surface region more heavily, was found to have only a small effect on the calculated ratio of π^- and π^+ cross sections.

In order to compare the strengths observed in the present work to those obtained with other probes, we followed the common procedure of comparing the measured cross section to a cross section normalized to exhaust the isoscalar linearly-energy-weighted sum rule. For $l \geq 2$, the $(\beta R)^2$ to exhaust the isoscalar sum rule is

$$(\beta R)_0^2 = \frac{\hbar^2}{2mA} \frac{4\pi}{\hbar\omega} \frac{l(2l+1)^2}{(l+2)^2} \frac{\langle r^{2l-2} \rangle}{\langle r^{l-1} \rangle^2} \, , \qquad (4)$$

where m is the nucleon mass and $\hbar\omega$ is the excitation energy of the state. The isospin nature of the sum rule is determined by the distribution used to compute the radial moments. The isoscalar sum rule, Eq. (4), is evaluated using the sum of identical neutron and proton ground state distributions. The electromagnetic sum rule would use the proton distribution alone.

To compare (βR)'s and sum rule fractions to other probes, the radial moments were evaluated for a uniform distribution, $\rho = 3/(4\pi R_0^3)$. Use of Woods-Saxon distributions for the ground states would raise the $(\beta R)_0^2$ to exhaust the $l = 2$ sum rule by a factor of 1.13 for ^{40}Ca and 1.09 for ^{118}Sn. We used $R_0 = 1.2A^{1/3}$ for both targets.

For the isovector giant dipole resonance, we used the Goldhaber-Teller model sum rule,[23] which, for a uniform density is

$$(\beta R)_1^2 = \frac{16\pi}{\hbar\omega} \frac{NZ}{A} \frac{\hbar^2}{2m} \quad (l = 1) \, . \qquad (5)$$

For the monopole resonance, the definition of the transition density we used implies that the normalization parameter is only β, not (βR). For 100% of the monopole isoscalar sum rule,[23] again assuming a uniform ground state density,

$$\beta^2 = \frac{4\pi}{\hbar\omega} \frac{\hbar^2}{2m^2} \frac{1}{A} \frac{5}{3R_0^2} \quad (l = 0) \, . \qquad (6)$$

The pion transition strengths extracted in this work can be compared to other probes either by comparison of sum rule fractions or of (βR)'s, where $(\beta R)^2$ is measured in the usual collective model way as $(\beta R)^2 = \sigma_{\text{meas}}/\sigma_{\text{calc}}$, and σ_{calc} is calculated including the $(Z - N)$ isovector interaction for B_1. These comparisons must be made carefully, however, because of the different nature of each probe's interaction with the nucleus. For example, the pion, which interacts both through isoscalar and isovector operators, will be compared to the alpha particle, which is a purely isoscalar probe. To do this we can extract the isoscalar and isovector deformation lengths. At energies near the $\Delta(1232)$ resonance, we can write

$$(3Z + N)(\beta R)_+ = 2(Z + N)(\beta R)_0 + (Z - N)(\beta R)_1 \, ,$$

$$(Z + 3N)(\beta R)_- = 2(Z + N)(\beta R)_0 - (Z - N)(\beta R)_1 \, ,$$

where $(\beta R)_\pm$ are the deformations measured using $\pi^\pm$, and $(\beta R)_{0,1}$ are the isoscalar and isovector deformations. Similarly, to compare to electron scattering we need the proton deformation which is found by solving

$$(3Z + N)(\beta R)_+ = 3Z(\beta R)_p + N(\beta R)_n \, ,$$

$$(Z + 3N)(\beta R)_- = Z(\beta R)_p + 3N(\beta R)_n \, ,$$

where $(\beta R)_{p,n}$ are the proton and neutron deformations. An alternate method of comparison, proposed by Bernstein, Brown, and Madsen,[26] will be discussed later.

IV. LOW-LYING COLLECTIVE STATES

Data on the low-lying collective states were taken for two reasons. First, they provide information on the π^-/π^+ ratio for standard collective states to compare to the giant resonances. Data for this comparison in the same nucleus have not previously been available. Second, the low-lying states are in a region of little continuum background and have been well studied with a number of different probes. This lets us compare the magnitudes of the deformation parameters extracted in the present work to previously existing data, using the transformations of Sec. III.

All the data on low-lying states were taken during the second run. The ^{118}Sn data were taken with the spectrometer tuned to put the low-lying states on a favorable region of the focal plane, while the ^{40}Ca data were taken at the same time as the giant resonances, missing the strong first 3^- state. Because we were primarily interested in giant resonances, the targets were thick and only a coarse angular distribution was taken.

Figure 2 shows the low-lying region in ^{118}Sn$(\pi^+,\pi^+{}')$ at 30°. The ground state, 2^+ at 1.23 MeV, and 3^- state at 2.31 MeV were fit simultaneously with Gaussian peak shapes with a skew to account for the tails. The overall resolution, dominated by the target thickness, was about 0.6 MeV. The 2^+ state is therefore well resolved from neighboring states, while the 3^- state is not. States near the 3^- peak were only weakly excited in low-energy proton scattering,[27] for example, and are not expected to contribute significantly to the observed 3^- peak. At scattering angles 17° and forward these states could not be resolved from the elastic tail.

The angular distributions for elastic scattering from ^{118}Sn are shown in Fig. 4. Calculations were made using DWPIES with only a first-order optical potential and no
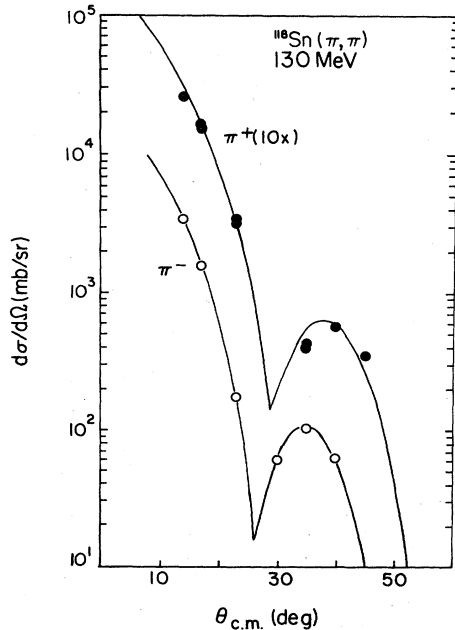
energy shift. The elastic data are well reproduced by the calculations, which confirms our assumption of equal ground state neutron and proton distributions.

The angular distributions for the 2^+ and 3^- states are shown in Fig. 5. Deformation lengths $(\beta R)_\pm$ were extracted as described in Sec. III. Table I shows the resulting $(\beta R)_\pm$ values compared to some representative values measured using other probes. We note that the (βR) values for π^+ and π^- are roughly equal to each other and comparable to, although larger than, those measured with other probes. A similar observation on the near equality of $\pi^\pm$ scattering to low-lying states in ^{28}Si, ^{58}Ni, and ^{208}Pb was made by Olmer et al.[3]

When expressed as an isospin strength, as described in Sec. III, the present pion data yield isoscalar deformations, $(\beta R)_0$, of 0.86 ± 0.08 fm for the first 2^+ state and 1.00 ± 0.09 fm for the first 3^- state. Both results are a bit larger than found by isoscalar probes for ^{120}Sn.[28,31] The proton deformations calculated for the two states are 0.82 ± 0.08 fm and 0.98 ± 0.09 fm, exceeding the results from electric probes[29,30] for the 2^+ state, but in agreement with the strength to the 3^- state.

Bernstein, Brown, and Madsen[26] have pointed out an alternative way of describing the probe dependence of the βR values. They parametrize the observed βR's in terms of the ratio of coupling strengths of an individual probe to the neutrons and protons in the nucleus, b_n/b_p, and the ratio of neutron to proton transition matrix elements, M_n/M_p, which presumably is a function only of nuclear structure and is independent of the probe. Figure 6 shows the (βR)'s for the 2^+ and 3^- states from Table I plotted as a function of b_n/b_p. The curve for the 2^+ transition is a theoretical calculation using the "no-parameter shell model" value[12] for the ratio of neutron to proton matrix

FIG. 4. Elastic scattering cross sections for ^{118}Sn. Curves are first order DWIA calculations with no energy shift.
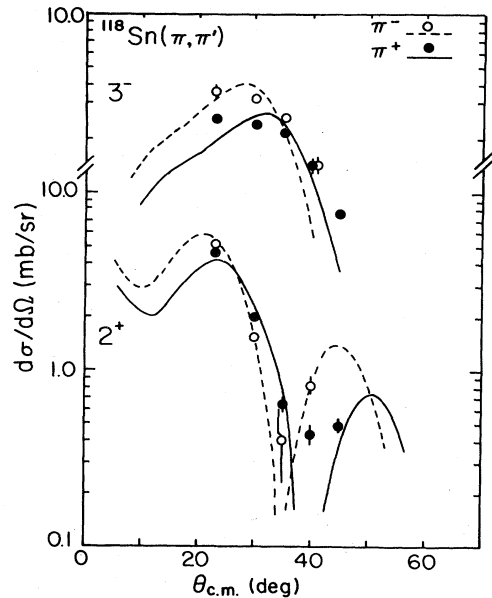

FIG. 5. Angular distributions for the first 2^+ state at 1.23 MeV, and the first 3^- state at 2.31 MeV, in ^{118}Sn. Uncertainties are statistical only.

TABLE I. Comparison of deformation length $(\beta R)_i$ for inelastic scattering on ^{118}Sn, in fm.

Probe		b_n/b_p	2^+ (1.23 MeV)	3^- (2.31 MeV)
π^+ 130 MeV $(\beta R)_+$	This work	0.33	0.84±0.08	0.99±0.09
π^- 130 MeV $(\beta R)_-$	This work	3.0	0.87±0.08	1.01±0.09
p 16 MeV	Ref. 27	3.0	0.78±0.06	0.99±0.06
p 800 MeV $(\beta R)_0$ (^{120}Sn)	Ref. 28	0.83	0.73	0.86
Coulomb excitation $(\beta R)_p$	Ref. 29	0.0	0.69±0.01	
Electron $(\beta R)_p$	Ref. 30	0.0	0.64	0.92
α 152 MeV $(\beta R)_0$ (^{120}Sn)	Ref. 31	1.0	0.65	0.73
n 11 MeV	Ref. 32	0.33	0.64±0.04	1.02±0.14
Derived quantities from the present work				
$(\beta R)_0$			0.86±0.08	1.00±0.09
$(\beta R)_1$			1.05±1.00	1.13±1.00
$(\beta R)_n$			0.88±0.08	1.02±0.09
$(\beta R)_p$			0.82±0.08	0.98±0.09

elements, $M_n/M_p = 1.68$, normalized to the Coulomb-excitation value. For the 3^- state the data from the different probes are compared to the hydrodynamic model prediction of a straight line.

For both states, the deformations βR are near the expected curves except for the 800 MeV proton and 152 MeV alpha scattering points. Both of these are for ^{120}Sn, not ^{118}Sn, and were at much higher momentum transfer than the other points. These consistencies have also been discussed by Finlay *et al.*[32]

Data were taken on the low-lying states in Ca above about 6 MeV in excitation, but were limited somewhat by poor statistics and incomplete angular distributions, due in part to hydrogen contamination on the target. Some

useful quantitative information can be obtained, however. Higher resolution pion scattering data to the 6.58 MeV 3_3^- state and below are available.[33,34] A sample Ca spectrum is shown in Fig. 1. Four states, with energies measured at 6.25, 6.90, 7.98, and 8.6 MeV were studied. Peak areas were extracted by simultaneously fitting the peaks with Gaussians constrained to have the same width. Table II shows the resulting deformation lengths compared to measurements made with other probes. Angular distributions are shown in Fig. 7.
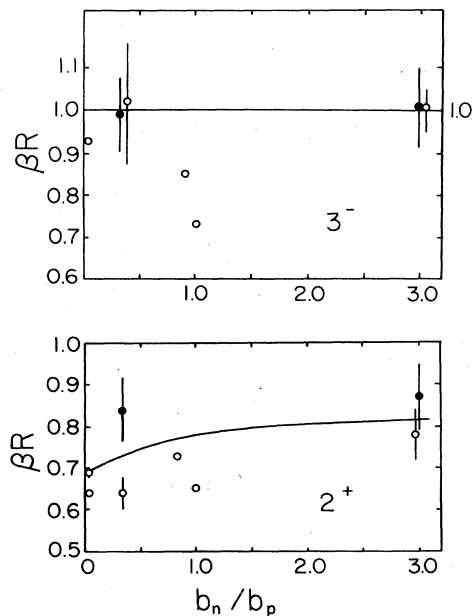

FIG. 6. Deformation length βR as a function of probe-nucleon coupling, b_n/b_p, for the first 2^+ and 3^- states in ^{118}Sn. Closed dots are the current measurements, open circles are measurements with other probes tabulated in Table I.
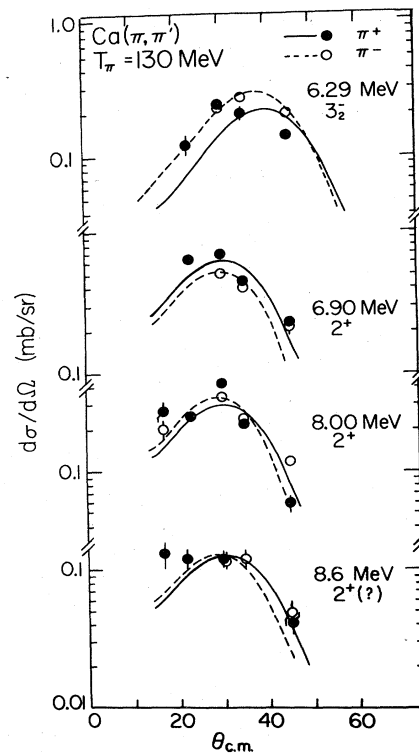

FIG. 7. Angular distributions for several low-lying 2^+ and 3^- states in Ca(π,π').

TABLE II. Ca deformation lengths βR in fm. The transformations of Sec. III have been used to convert the pion results to isoscalar or charge (proton) deformations.

E_x l transfer		6.29 MeV 3	6.94 MeV 2	8.00 MeV 2	8.6 MeV 2
π^+ 130 MeV $(\beta R)_+$	This work	0.44±0.05 fm	0.49±0.05 fm	0.33±0.04 fm	0.22±0.02 fm
π^- 130 MeV $(\beta R)_-$	This work	0.45±0.05	0.41±0.05	0.32±0.04	0.20±0.02
p 800 MeV $(\beta R)_0$	Ref. 36	0.38	0.49		
p 30 MeV	Ref. 37	0.43	0.43	0.42	0.32
α 120 MeV $(\beta R)_0$	Ref. 35	0.36		0.50	0.42
Derived quantities					
$(\beta R)_0$	This work	0.45	0.45	0.33	0.21
$(\beta R)_p$	This work	0.44	0.53	0.34	0.23

The first state is identified as the 6.29 MeV 3_2^- state studied by Morris et al.[33] and Boyer et al.[34] with better resolution. Our data are consistent with their 116 MeV data. The region of excitation near 7 MeV is becoming dense in states, and a strong state at about 6.94 MeV has been variously identified as a 2^+ or 3^- level. Our angular distribution favors the 2^+ interpretation, and in Table II we compare to other data that are consistent with an $l=2$ transition. The strong 3_3^- state at 6.58 MeV studied by Morris et al.[33] and Boyer et al.[34] is much weaker than the 2^+ state at the energy and momentum transfer of this experiment. Near 8 MeV in excitation, $l=4$ states have been reported,[35-37] but their contribution to our data is again small. Alpha scattering data[35] show two strong 2^+ states at 7.90 and 8.10 MeV, which we sum together to compare to our peak at 8.00 MeV, which is consistent with a 2^+ interpretation.

Finally, the weak peak we observe at 8.6 MeV is tentatively associated with a cluster of two or three 2^+ states reported in alpha[35] and proton[37] scattering. The summed strength of the cluster is shown in Table II.

As seen in Fig. 7, the DWIA calculations are quite reasonable for the assumed spin values. The isoscalar and proton deformations for these four states are listed in Table II. There are significant differences from the values for purely isoscalar probes. However, for all states we note that the ratio $(\beta R)_+/(\beta R)_-$ is very close to unity, consistent with a pure isoscalar response in an $N=Z$ nucleus.

V. GIANT RESONANCE REGION

A. Ca

As described in Sec. II, the giant resonance region in ^{40}Ca cannot be fit by simple Gaussian shapes, and the region was treated as a complex. The GQR is expected to be centered at about 18 MeV (Ref. 19) and the giant dipole resonance at about 20 MeV.[38] The isoscalar monopole resonance is also expected to lie in this region on the basis of energy systematics.[6] While measurements of the monopole strength run as high as 250% of the monopole sum rule,[39] a very careful study of the region using the (α, α') reaction[19] yielded no evidence for a compact mono-

pole structure. Similar results were also obtained in ^{40}Ca(p,p') at 60 MeV,[40] and for this reason we do not consider monopole strength.

The angular distributions for the giant resonance complex are shown in Fig. 8. We see that an $l=2$ curve alone does not adequately characterize the data at forward angles, and an $l=1$ contribution must be included. The π^- data were fit by a combination of 30% of the energy-weighted sum rule for the GQR plus 100% of the giant dipole sum rule, the π^+ data by 27% of the GQR plus 135% of the giant dipole sum rules. (See Table III.) The measured cross section ratio at 35°, where the dipole contribution is small, is $\pi^-/\pi^+=1.05\pm0.28$. The large uncertainty is due to the assumed 20% uncertainty in the estimation of each peak area. The calculated cross section
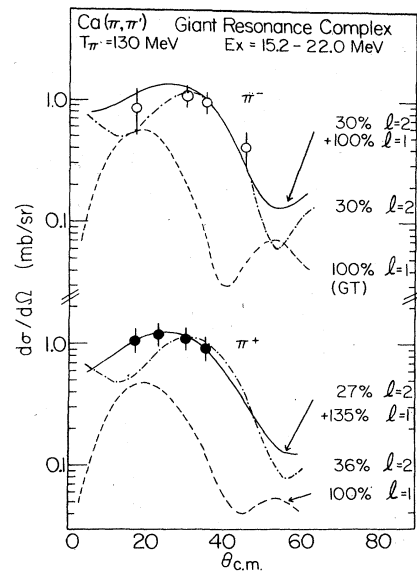

FIG. 8. Angular distributions for the giant resonance region in ^{40}Ca, $E_x=15.2-22.0$ MeV. Open circles are π^- data, closed are π^+. Continuous curves represent the results of fitting a sum of $l=2$ (GQR) and $l=1$ (GDR) curves to the data. The dot-dashed curves are the result of fitting only a GQR contribution, and the dashed curves show the giant dipole strength normalized to 100% of the Goldhaber-Teller sum rule.

TABLE III. Isoscalar giant resonance sum rules. The transformations of Sec. III have been used to convert the pion strengths. In a hydrodynamic model, the isoscalar and isovector strengths should be the same.

Description			% energy-weighted sum rule		
			Ca		
			GQR	GDR	
$Ca(\pi^-,\pi^{-\prime})$	130 MeV	This work	30	100	
$Ca(\pi^+,\pi^{+\prime})$	130 MeV	This work	27	135	
$Ca(\pi^+,\pi^{+\prime})$	163 MeV	Ref. 8	60	150	
$Ca(\alpha,\alpha')$	117 MeV	Ref. 19	(48±8)		
$Ca(p,p')$	60 MeV	Ref. 40	(40±10)		
$^{40}Ca(e,e')$		Ref. 41 13—19 MeV excitation	47		
$^{40}Ca(^3He,^3He')$	109 MeV	Ref. 42	34		
			^{118}Sn		
			LEOR	GQR	GMR
$^{118}Sn(\pi^-,\pi^{-\prime})$	130 MeV	This work	(19±2)	(57±6)	(140±14)
$^{118}Sn(\pi^+,\pi^{+\prime})$	130 MeV	This work	(19±1)	(37±3)	(73±7)
$^{118}Sn(\alpha,\alpha')$	129 MeV	Ref. 17		60	150
$^{118}Sn(\alpha,\alpha')$	115 MeV	Ref. 43	20		
$^{120}Sn(\alpha,\alpha')$	129 MeV	Ref. 17		80	180
$^{120}Sn(\alpha,\alpha')$	152 MeV	Ref. 31		70	100
$^{120}Sn(p,p')$	200 MeV	Ref. 44		35	
$^{116}Sn(e,e')$	(Tassie FF)	Ref. 45		65	
$^{116}Sn(p,p')$	800 MeV	Ref. 46	(25±8)		
$^{116}Sn(^3He,^3He')$	120 MeV	Ref. 47	(25±3)		
Derived quantities (this work)					
^{118}Sn isoscalar			(19±2)	(47±4)	(106±10)
^{118}Sn isovector			(19±15)	(270±140)	(1010±400)
^{118}Sn proton			(19±2)	(35±3)	(41±5)
^{118}Sn neutron			(19±2)	(66±7)	(173±17)

ratio is also 1.05, so the π^-/π^+ ratio for the GQR contribution seems to be well represented by the calculations.

The $^{40}Ca(\pi^\pm,\pi^{\pm\prime})$ reaction to the giant resonance region has been previously studied at 163 and 241 MeV by Buenerd and Arvieux,[8] although only π^+ cross sections have been quoted. At 165 MeV, they observed data that corresponded to 60% of the GQR sum rule plus 150% of the giant dipole sum rule. Sum rule fractions for the GQR obtained using other probes are summarized in Table III. A more complete table has been published by Liu et al.[19] containing also alpha scattering results at other energies. We observed that the sum rule fractions for the GQR that we measure, when expressed as isoscalar or proton strength, are smaller than observed by other probes and in the previous pion experiment, although there seems to be considerable scatter in the values due to the unresolved nature of the peak. The sharply structured angular distributions for pion scattering make the separation of the multipolarities seem reliable for the pion probe.

Accurate determination of the giant dipole strength is difficult since its contribution to the measured cross section is considerably smaller than that of the giant quadrupole. The result of our fitting procedure is to estimate that 100% of the giant dipole Goldhaber-Teller sum rule is exhausted by π^- scattering, and 135% by π^+. This can be compared to the work of Buenerd and Arvieux,[8] who estimated that 150% of the dipole sum rule is found in π^+ scattering at 163 and 241 MeV. The giant dipole strength measured by photoabsorption over the energy range of 10 to 25 MeV is 130% of the Thomas-Reiche-Kuhn (TRK) sum rule,[38] near that observed for the proton strength (Table III) derived from the pion data.

An additional comparison of the giant dipole data can be made to $^{40}Ca(\pi^\pm,\pi^0)$ measurements of the analog dipole state made by Erell et al.[48] at 165 MeV. The charge exchange channels in $T=0$ nuclei are sensitive only to isovector transitions, so only the giant dipole and isovector monopole modes should contribute to this region of excitation. Naively, by assuming isospin invariance, the strengths for the charge exchange and inelastic channels should be equal. However, as pointed out by Auerbach and Klein,[49] the Coulomb shift of the giant dipole between charge exchange and inelastic modes can result in nontrivial differences in the giant resonance transition density, making naive quantitative comparisons problematic. Auerbach[50] has observed that because of

Coulomb repulsion, in a self-conjugate nucleus such as ^{40}Ca, there should be a slight proton excess at the nuclear surface. This results in the proton transition density extending slightly farther than the neutron density, implying that the (π^-, π^0) cross section should be greater than the (π^+, π^0) cross section. For inelastic scattering, similar arguments would predict the $(\pi^+, \pi^{+'})$ strength to be greater than the $(\pi^-, \pi^{-'})$, strength. Both reactions consistently find a small effect as expected for such a greater proton radius.

B. ^{118}Sn

An acceptance-corrected spectrum of the giant resonance region in ^{118}Sn is shown in Fig. 3. The low energy octupole resonance (LEOR) is a very clear peak with a maximum cross section at about 5.4 MeV excitation. The region containing the giant quadrupole resonance at 13.2 MeV and the giant dipole resonance at 15.6 MeV was analyzed by assuming two Gaussian shapes, as described in Sec. II. The sum rule strengths for each resonance are summarized in Table III, which also shows a comparison to sum rules measured by other probes in ^{118}Sn, or in ^{116}Sn or ^{120}Sn where ^{118}Sn data are not available. Except as noted, all sum rule strengths were calculated by a least-squares fit of the data to calculations made using a derivative collective transition density and $Z - N$ weighting for B_1 as described in Sec. III. The pion sum rule fractions were then converted to proton sum rule fractions, using the relations for βR in Sec. III, to compare to other probes.

The peak area for the LEOR was determined by summing counts over a straight line background from 4.6 to 8.4 MeV in excitation. The region is consistent with that analyzed in alpha scattering.[43] The angular distribution is shown in Fig. 9. At more forward angles the data do not

agree well with a pure $l = 3$ excitation, and there is evidence that other states may contribute at these lower momentum transfers.

The ratio of π^-/π^+ cross sections for the LEOR from the second run at 30° is 1.5 ± 0.4, which can be compared to the calculated ratio of 1.41. As shown in Table II, both π^+ and π^- scattering exhaust 19% of the $l = 3$ energy-weighted sum rule. When expressed in terms of the isoscalar sum rule, this is consistent with the alpha-scattering results. However, the derived proton sum rule fraction is not consistent with electron scattering results on ^{116}Sn.

The angular distributions we obtained for the isoscalar giant quadrupole resonance are shown in Fig. 10. The data show good consistency between the two runs so only the weighted average of the two runs is shown at overlap points. These data have been published in a previous Letter.[2] The angular distribution is described well by the $l = 2$ shape. Bertrand et al.[44] have placed an upper limit of 5% EWSR for an $l = 4$ giant resonance predicted to occur near the giant quadrupole. This state could make a contribution near the minimum of the cross section, but would not affect our sum rule fraction or interpretation. The ratio $\sigma(\pi^-)/\sigma(\pi^+)$ of the cross sections at 23° is 1.9 ± 0.4. For comparison, the cross section ratio for the first 2^+ state discussed in Sec. IV is 1.1 ± 0.1. When expressed as an isoscalar strength, the pion GQR data yield $(47 \pm 4)\%$ of the isoscalar sum rule, a bit below that found in alpha particle scattering.[19] The pion proton strength is also below that found in electron scattering.[45]

The results for the giant monopole-dipole region are shown in Fig. 11. The data are consistent with a monopole excitation, based on a comparison with the calculated angular distributions which show sharply peaked $l = 0$ structure. The π^-/π^+ ratio of the weighted average of the 30° cross sections is 2.27 ± 0.52. The ratio of DWIA cross sections for π^-/π^+ at 30°, using the hydrodynamic
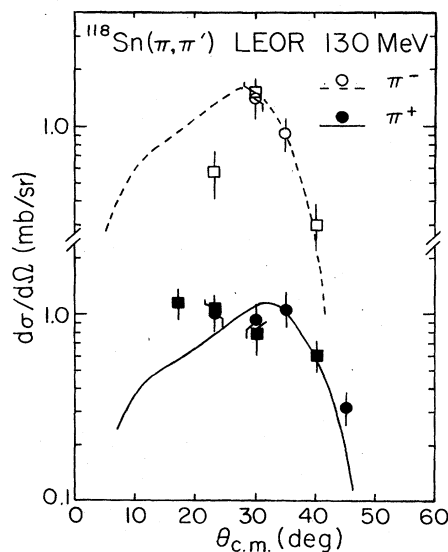
FIG. 9. Angular distributions for the low-energy octupole resonance (LEOR) in ^{118}Sn. Circles are data from the second run, squares from the first run.
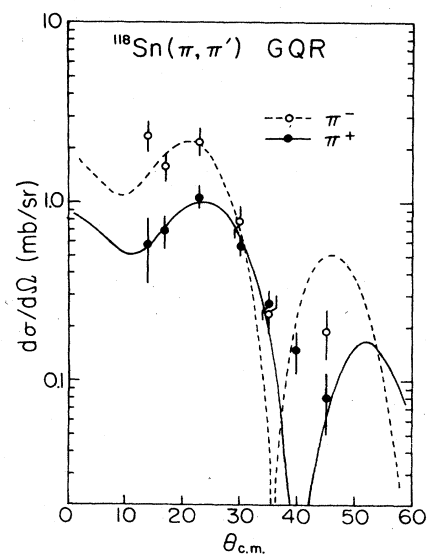
FIG. 10. Angular distributions for the giant quadrupole resonance in ^{118}Sn. The weighted averages of data from the first and second runs are shown.
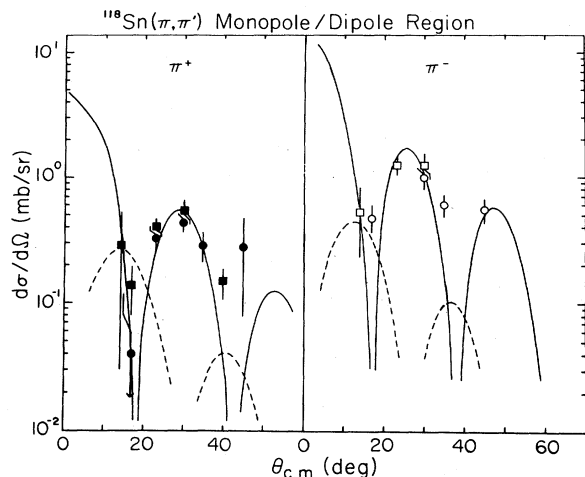
FIG. 11. Angular distributions for the giant monopole-dipole region in ^{118}Sn. The squares are data from the first run, the circles from the second. Solid lines are the result of fitting only a monopole calculation to the data. The dashed lines are the expected dipole contribution normalized as described in the text.

N/Z weighting of neutrons and protons, is 1.00. The sum rule fraction exhausted in π^- scattering is $(140\pm14)\%$, and in π^+ is $(73\pm7)\%$ for a π^-/π^+ strength ratio of 1.92 ± 0.27. This is similar to the ratio observed for the GQR. From Table III, we see that the derived isoscalar strength agrees with some alpha scattering results.

A contribution from the giant dipole resonance is expected since photonuclear measurements of its strength show it exhausts 107% of the classical (TRK) sum rule.[18] The giant dipole resonance has been studied in ^{120}Sn(π^+,π^0) at 165 MeV,[51] so we elected to compare our cross sections to their data. As noted previously, the comparison of giant resonance strengths between charge exchange and inelastic channels involves nontrivial calculations of strength that are model dependent. For this reason, this comparison must be considered at best a rough qualitative consistency check.

We first scaled the 165 MeV charge-exchange cross sections to 130 MeV by the ratio of DWIA calculations at the first maximum. Next the $\Delta\tau=-1$, cross sections are scaled to the $\Delta\tau=0$ channel by the ratio of the "zero moment" of the strengths calculated by Auerbach and Klein (see Table 4 of Ref. 49). Dipole angular distributions normalized to this value are shown as broken lines in Fig. 11. We note that the dipole contribution might be observed only in the deep minima of the monopole distribution. Our data are consistent with this picture.

We observe that the ratio of π^- to π^+ cross sections to the continuum region above the giant monopole (20 to 26 MeV in excitation) is 1.90 ± 0.15, evidence for a neutron-like enhancement as found for the unbound giant resonances.

VI. DISCUSSION

The most interesting result of this experiment is the large difference observed between π^+ and π^- inelastic scattering cross sections to the isoscalar giant quadrupole and giant monopole resonances in ^{118}Sn, while the low energy octupole resonance and the first 2^+ and 3^- states do not exhibit this asymmetry. On the other hand, no major difference is observed in inelastic scattering to either the giant quadrupole resonance or the low-lying states in the self-conjugate nucleus ^{40}Ca.

The extreme shell model picture of isoscalar collective states predicts that shell structure should be important in the $0\hbar\omega$ collective states. The first 2^+ state in a closed proton shell nucleus such as ^{118}Sn should be primarily a neutron vibration; this should favor π^- inelastic scattering over π^+. In practice, there are large core polarization contributions from the mixing of the giant quadrupole resonance with the lower states, reducing the difference considerably.[26,12]

The $0\hbar\omega$ collective states in single closed-shell nuclei have been the subject of extensive studies by Bernstein, Brown, and Madsen.[26] They have presented a unified description of inelastic scattering to these states by many hadronic and electromagnetic probes, relating the observed deformation lengths to the properties of the probe-nucleon interaction and the neutron or proton multipole matrix elements. The results in the Sn region, which predict that the π^- deformation length for the first 2^+ state should be about 10% larger than for π^+, seem to be in agreement with experiment.[26] The data we have presented for the first 2^+ state are consistent with a small π^- enhancement.

The isoscalar giant resonances involve particle-hole excitations across one or more major shells. In the $2\hbar\omega$ giant quadrupole resonance, for example, the shell effects in this picture should be minimal, and any differences between the π^- and π^+ cross sections should be due only to the numerical excess of neutrons able to participate in a $2\hbar\omega$ excitation.

In comparing our data to macroscopic theories we require that no fine structure exists within a giant resonance. The giant resonances are in fact composed of many states, and random-phase approximation (RPA) solutions sometimes have rather extreme ratios of neutron and proton matrix elements for individual components of the resonance. Because we are seeing only about 50% of the $E2$ sum rule strength in a lumped resonance, there could be additional $E2$ strength lurking in the continuum. This hidden strength taken together with the lumped resonance might exhibit different properties. We assume here, however, that the portion of the resonance we observe is representative of the entire resonance strength, as used in other analyses of data.

We have concentrated our attention on understanding the π^-/π^+ ratio observed for the giant quadrupole resonance, and have made calculations based on several different macroscopic approaches. All calculations were based on the derivative transition density of Eq. (2) and used $B_0 = Z(\beta R)_p + N(\beta R)_n$. Initially we set $(\beta R)_p = (\beta R)_n = (\beta R)_0$, a deformation parameter determined to exhaust the sum rule. We first considered the giant quadrupole resonance to be a pure isoscalar response and set $B_1 = 0$. This implies that the π^- and π^+ cross sections can differ only because of differences in the distorted

waves. This cross section difference was calculated to be 5% near the maximum, which is far less than we observed. Next we assumed the hydrodynamical model and set $B_1 = Z(\beta R)_0 - N(\beta R)_0$. This yielded a π^-/π^+ cross section ratio of 1.35, which, although larger than unity, is still less than the observed value of 1.9.

We also used the schematic model results of Brown and Madsen[12] which allow $(\beta R)_p$ and $(\beta R)_n$ to differ. Their results are expressed in terms of the ratio of neutron to proton transition matrix elements, $M_n/M_p = N(\beta R)_n/Z(\beta R)_p$. For the GQR in ^{118}Sn their model predicts[13] $M_n/M_p = 1.23$ yielding a cross section ratio at 23 deg of 1.23, which is again quite different from the measured value. We can obtain a value of M_n/M_p directly from the data by noting that at 23 deg the effects of distortions on π^+ and π^- are nearly equal. In this situation, the cross section ratio goes like the square of Eq. (1) and yields the approximate result $M_n/M_p \approx \sigma(\pi^-)/\sigma(\pi^+)$. This implies that $M_n/M_p \approx 1.9 \pm 0.4$. A similar value of $M_n/M_p = 2.08$ was obtained by Kailas et al.[52] in a study of inelastic proton and alpha scattering in ^{120}Sn.

The pion results, when expressed as isoscalar or proton strengths, are in general not beyond agreement with the results of other probes, considering the scatter in the reported results. Using the relations in Sec. III, the rarely-probed isovector and neutron strengths can also be derived from our data. In these terms, larger fractions of the neutron than proton sum rule are exhausted for the GQR and GMR, but the same fractions are found for the LEOR. In terms of isospin, large fractions of the isovector sum rule are exhausted in the GQR and GMR, but not the LEOR.

Our results for the GQR and GMR in ^{118}Sn imply the need for large isovector contributions to transitions considered to be primarily isoscalar. However, before considering arguments involving isospin impurities, we will try to understand our observations in more conventional terms. Pions at energies near the $\Delta(1232)$ resonance are strongly absorbed and therefore sensitive only to features on the surface of the nucleus. It is possible that small surface differences in the neutron and proton transition densities, which were assumed to have equal shapes, might strongly affect the calculations. To test this, derivative transition densities based on different realistic neutron and proton densities[53,54] were tried, but only a 2% effect was observed. We also tried a Tassie[25] form of the transition density, $\rho \approx r^{l-1} \rho'_{g.s.}$, which weights the surface region more heavily. This method predicted a cross section ratio at 23° of 1.38 which is virtually the same as obtained using Eq. (2). This is not surprising since even though we are weighting the surface more, we are still assuming equal neutron and proton shapes with N and Z weighting. The ratio N/Z is 1.36 for ^{118}Sn.

Another effect, whose importance in comparing π^+ and π^- scattering has been recently pointed out by Siciliano and Weiss,[55] must also be considered. They observe that for states located well above particle threshold, surface differences between the neutron and proton wave functions must be considered. The neutron and proton separation energies for ^{118}Sn are 9.33 and 10.01 MeV, respectively, so the giant quadrupole and monopole resonances are

both above particle threshold, while the LEOR is not. For inelastic scattering of pions at energies near the Δ resonance (130 MeV is sufficiently close) it has been shown[56] that the scattering may be considered to take place at a strong absorption radius of about $1.4A^{1/3}$ fm. Thus, π^-/π^+ asymmetries resulting from differences in the neutron and proton wave functions near this point, which is in the far tail region of the transition density, must be considered. The need to consider the unbound nature of the wave functions is emphasized by observing that the π^-/π^+ cross section ratio for the LEOR, which is below particle threshold, is exactly as expected from the DWIA calculations, while the π^-/π^+ ratio for the unbound GQR and isoscalar giant monopole resonances both exhibit the large π^-/π^+ ratio.

Although simple calculations using "typical" unbound single-particle wave functions to form the transition density reproduce qualitatively the π^-/π^+ ratio observed for the GQR,[57] giant resonances are complicated sums over many particle-hole states and must be treated carefully to get quantitative results. Most RPA calculations of GQR transition densities have been made using a harmonic oscillator basis for the wave functions, and do not predict the surface effects due to the unbound nature of the transition. Auerbach and Klein have done extensive continuum RPA calculations for isovector giant resonances.[49] In addition, Auerbach, Klein, and Siciliano have recently considered pion scattering to the isoscalar resonances.[58]

A different explanation of the π^-/π^+ ratio has been proposed by True and King[59] in a valence-nucleon collective picture. They assume $(\beta R)_n = (\beta R)_p$, but allow the effective number of neutrons and protons to vary, yielding a M_n/M_p different from hydrodynamic value. While $2\hbar\omega$ excitations are expected to be relatively insensitive to the details of shell structure, by fitting the available data the effective number of neutrons and protons was found to correlate well with the number of nucleons outside the next lower filled shell or subshell. This study has examined a large pion data set for low-lying collective states to arrive at a correlation between shell structures and π^-/π^+ strengths. Variations in neutron and proton radial distributions and isospin mixing arguments were also investigated as possible explanations for the large observed ratios.

If the unbound effects provide the explanation of the observed ratio, the results will in one sense be disappointing, because surface effects which are rather difficult to calculate will mask the microscopic isospin nature of the transition. We will have to distinguish carefully between an isoscalar excitation, a purely nuclear structure feature, and an isoscalar experimental result, which will reflect the sensitivity of different probes to the nuclear surface.

VII. SUMMARY

The first 2^+ and 3^- states have been studied in ^{118}Sn and several well-known low-lying 3^- and 2^+ states have been observed in Ca. In Ca, the deformation lengths for π^+ and π^- are for the most part equal within the statistical accuracy of the measurement and comparable to deformation lengths measured with other probes after the appropriate transformations. In ^{118}Sn, the deformation

lengths for π^+ and π^- scattering to the 3^- state are equal and in reasonable agreement with other probes. The deformation lengths for the 2^+ state are roughly equal but consistent with an expected slight π^- enhancement.

In ^{40}Ca, the giant isoscalar quadrupole and isovector dipole resonances are observed as an unresolved complex. The angular distributions are reasonably well characterized, considering there are only four points each for π^+ and π^-. The GQR sum rule fractions for π^+ and π^- are roughly equal, but after transforming to proton or isoscalar terms these fractions are somewhat lower than observed using other probes. The sum rule fraction for the giant dipole was poorly determined, but roughly consistent with other probes.

In ^{118}Sn, the giant resonance region was resolved into a giant quadrupole peak and an isoscalar monopole plus iso-

vector dipole peak. The low energy octupole resonance was also observed. We observed a π^-/π^+ sum rule ratio of 1.54 ± 0.29 for the quadrupole, 1.92 ± 0.38 for the monopole, and 1.00 ± 0.16 for the LEOR.

This work has demonstrated that pion scattering experiments using both charge states yield transition strengths roughly comparable to results using other probes, but in addition yield information on isovector or neutron strengths which are difficult to examine by other means. The observed large π^-/π^+ ratio for the GQR and GMR implies the need for a strong isovector amplitude or alternately, a large neutron amplitude. This result cannot be understood using the usual collective model approach. It reflects the need to understand the surface features of the reaction in detail, and perhaps suggests a sensitivity to the unbound nature of the excitation.

*Present address: University of Michigan Group, Brookhaven National Laboratory, Upton, NY 11973.

†Present address: Rockwell International, Golden, CO 80401.

‡Present address: University of Georgia, Athens, GA 30602.

[1]C. L. Morris, Phys. Rev. C **13**, 1755 (1976).

[2]J. L. Ullmann, J. J. Kraushaar, T. G. Masterson, R. J. Peterson, R. S. Raymond, R. A. Ristinen, N. S. P. King, R. L. Boudrie, C. L. Morris, W. W. True, R. E. Anderson, and E. R. Siciliano, Phys. Rev. Lett. **51**, 1038 (1983).

[3]C. Olmer *et al.*, Phys. Rev. C **21**, 254 (1980); K. G. Boyer *et al.*, *ibid.* **24**, 598 (1981).

[4]S. G. Iverson *et al.*, Phys. Rev. Lett. **40**, 17 (1978).

[5]C. A. Wiedner *et al.*, Phys. Lett. **78B**, 26 (1980).

[6]F. E. Bertrand, Nucl. Phys. **A354**, 129 (1981).

[7]J. Arvieux, J. P. Albanese, M. Buenerd, J. Bolger, E. Boschitz, G. Pröbstle, F. Vogler, K. Gabathuler, P. A. M. Gram, J. Jansen, and R. E. Mischke, Phys. Lett. **90B**, 371 (1980).

[8]J. Arvieux *et al.*, Phys. Rev. **42**, 753 (1979); M. Buenerd and J. Arvieux, *Giant Multipole Resonances*, edited by F. E. Bertrand (Harwood, New York, 1980), p. 381.

[9]L. C. Bland, Ph.D. thesis, University of Pennsylvania, 1984.

[10]C. F. Moore, C. J. Harvey, C. L. Morris, W. B. Cottingame, S. J. Greene, D. B. Holtkamp, and H. T. Fortune, Phys. Rev. C **26**, 2561 (1982).

[11]A. Bohr and B. R. Mottelson, *Nuclear Structure* (Benjamin, Reading, Mass., 1975), Vol. II, Chap. 6.

[12]V. R. Brown and V. A. Madsen, Phys. Rev. C **11**, 1298 (1975).

[13]V. A. Madsen, private communication.

[14]C. L. Morris (unpublished).

[15]T. G. Masterson, J. J. Kraushaar, R. J. Peterson, R. S. Raymond, R. A. Ristinen, R. L. Boudrie, E. F. Gibson, and A. W. Thomas, Phys. Rev. C **26**, 2091 (1982).

[16]Program SCATPI, written by B. Walter and G. A. Rebka, Los Alamos Report UC34A, 1979 (unpublished), based on the phase shifts of J. R. Carter, D. V. Bugg, and A. A. Carter, Nucl. Phys. **B58**, 378 (1973).

[17]D. H. Youngblood, P. Bogucki, J. D. Bronson, U. Garg, Y. W. Lui, and C. M. Rozsa, Phys. Rev. C **23**, 1997 (1981).

[18]B. L. Berman and S. C. Fultz, Rev. Mod. Phys. **47**, 713 (1975).

[19]Y. W. Lui, J. D. Bronson, C. M. Rosza, D. H. Youngblood, P. Bogucki, and U. Garg, Phys. Rev. C **24**, 884 (1981).

[20]R. A. Eisenstein and G. A. Miller, Comput. Phys. Commun. **11**, 95 (1976).

[21]G. Rowe, M. Salomon, and R. H. Landau, Phys. Rev. C **18**, 584 (1978).

[22]E. R. Siciliano and G. E. Walker, Phys. Rev. C **23**, 2661 (1981).

[23]G. R. Satchler, in *Elementary Modes of Excitation in Nuclei*, edited by A. Bohr and R. A. Broglia (North-Holland, Amsterdam, 1977). [See also Nucl. Phys. **A195**, 1 (1972)].

[24]C. W. deJager, H. deVries, and C. deVries, At. Data Nucl. Data Tables **14**, 479 (1974).

[25]L. J. Tassie, Aust. J. Phys. **9**, 407 (1956).

[26]A. M. Bernstein, V. R. Brown, and V. A. Madsen, Phys. Lett. **103B**, 255 (1981); **106B**, 259 (1981).

[27]W. Makofske, W. Savin, H. Ogata, and T. H. Kruse, Phys. Rev. **174**, 1429 (1968).

[28]M. M. Gazzaly, N. M. Hintz, G. S. Kyle, R. K. Owen, G. W. Hoffman, M. Barlett, and G. Blanpied, Phys. Rev. C **25**, 408 (1982).

[29]R. Graetzer, S. M. Cohick, and J. X. Saladin, Phys. Rev. C **12**, 1462 (1975).

[30]T. H. Curtis, R. A. Eisenstein, D. W. Madsen, and C. K. Bockelman, Phys. Rev. **184**, 1162 (1969).

[31]F. E. Bertrand, G. R. Satchler, D. J. Horen, J. R. Wu, A. D. Bacher, G. T. Emery, W. P. Jones, D. W. Miller, and A. Van der Woude, Phys. Rev. C **22**, 1832 (1980).

[32]R. W. Finlay, M. H. Hadizadeh, J. Rapaport, and D. E. Bainum, Nucl. Phys. **A344**, 257 (1980); R. W. Finlay, J. Rapaport, M. H. Hadizadeh, M. Mirzaa, and D. E. Bainum, *ibid.* **A338**, 45 (1980).

[33]C. L. Morris, K. G. Boyer, C. F. Moore, C. J. Harvey, K. J. Kallianpur, I. B. Moore, P. A. Seidl, S. J. Seestrom-Morris, D. B. Holtkamp, S. J. Greene, and W. B. Cottingame, Phys. Rev. C **24**, 231 (1981).

[34]K. G. Boyer, W. J. Braithwaite, W. B. Cottingame, S. J. Greene, L. E. Smith, C. F. Moore, C. L. Morris, H. A. Thiessen, G. S. Blanpied, G. R. Burleson, J. F. Davis, J. S. McCarthy, R. C. Minehart, and C. A. Goulding, Phys. Rev. C **29**, 182 (1983).

[35]K. Van der Borg, M. N. Harakeh, A. Van der Borg, M. N. Harakeh, and A. Van der Woude, Nucl. Phys. **A365**, 243

(1981).

[36]G. S. Adams, T. S. Bauer, G. Igo, G. Pauletta, C. A. Whitten, A. Wriekat, G. W. Hoffmann, G. R. Smith, and M. Gazzaly, Phys. Rev. C **21**, 2485 (1980).

[37]C. R. Gruhn, T. Y. T. Kuo, C. J. Maggiore, H. McManus, F. Petrovich, and B. M. Preedom, Phys. Rev. C **6**, 915 (1972).

[38]J. Ahrens, H. Borchert, K. H. Czock, H. B. Eppler, H. Grimm, H. Gundrum, M. Kroning, P. Richn, G. Sita Ram, A. Zieger, and B. Ziegler, Nucl. Phys. **A251**, 479 (1975).

[39]N. Marty, M. Morlet, A. Willis, V. Comparat, and R. Frascaria, Nucl. Phys. **A237**, 93 (1975).

[40]F. E. Bertrand, G. R. Satchler, D. J. Horen, and A. Van der Woude, Phys. Lett. **80B**, 198 (1979).

[41]Y. Torizuka, K. Itoh, Y. M. Shin, Y. Kawazoe, H. Matsuzaki, and G. Takeda, Phys. Rev. C **11**, 1174 (1975).

[42]D. LeBrun, M. Buenard, P. Martin, P. de Saintignon, and G. Perrin, Phys. Lett. **97B**, 358 (1980).

[43]J. M. Moss, D. R. Brown, D. H. Youngblood, C. M. Rosza, and J. D. Bronson, Phys. Rev. C **18**, 741 (1978).

[44]F. E. Bertrand, E. G. Gross, D. J. Horen, J. R. Wu, J. Tinsley, D. K. McDaniels, L. W. Swenson, and R. Liljestrand, Phys. Lett. **103B**, 326 (1981).

[45]K. Hosoyama and Y. Torizuka, Phys. Rev. Lett. **35**, 199 (1975).

[46]T. A. Carey, W. D. Cornelius, N. J. DiGiacomo, J. M. Moss, G. S. Adams, J. B. McClelland, G. Pauletta, C. Whitten, M. Gazzaly, N. Hintz, and C. Glashausser, Phys. Rev. Lett. **45**, 239 (1980).

[47]T. Yamagata, S. Kisihmoto, K. Yuasa, K. Iwamoto, B. Sacki, M. Tanaka, T. Fukuda, I. Miura, M. Inouc, and H. Ogata, Phys. Rev. C **23**, 937 (1981).

[48]A. Erell, J. Alster, J. Lichtenstadt, M. A. Moinester, J. D. Bowman, M. D. Cooper, F. Irom, H. S. Matis, E. Piasetzky, U. Sennhauser, and Q. Ingram, Phys. Rev. Lett. **52**, 2134 (1984).

[49]N. Auerbach and A. Klein, Nucl. Phys. **A359**, 77 (1983).

[50]N. Auerbach, Phys. Rev. Lett. **49**, 913 (1982).

[51]J. D. Bowman, H. W. Baer, R. Bolton, M. D. Cooper, F. H. Cverna, N. S. P. King, M. Leitch, H. S. Matis, A. Erell, J. Alster, A. Doron, M. A. Moinester, E. Blackmore, and E. R. Siciliano, Phys. Rev. Lett. **50**, 1195 (1983).

[52]S. Kailas et al., in *Proceedings of the International Conference on Nuclear Structure, Amsterdam, 1982,* edited by A. Van der Woude and B. J. Verhaar (European Physical Society, Petit-Lancy, Switzerland, 1982), p. 93.

[53]M. Beiner et al., Nucl. Phys. **A238**, 29 (1975).

[54]J. W. Negele and D. Vautherin, Phys. Rev. C **5**, 2472 (1972).

[55]E. R. Siciliano and D. L. Weiss, Phys. Lett. **93B**, 371 (1980).

[56]M. B. Johnson, Phys. Rev. C **22**, 192 (1980).

[57]J. L. Ullmann and R. J. Peterson, Bull. Am. Phys. Soc. **29**, 675 (1984).

[58]N. Auerbach, A. Klein, and E. R. Siciliano (unpublished).

[59]W. W. True and N. S. P. King (unpublished).